JCTC Journal of Chemical Theory and Computation

Article

Cite This: J. Chem. Theory Comput. 2018, 14, 1395−1402

pubs.acs.org/JCTC

Deterministic Construction of Nodal Surfaces within Quantum Monte Carlo: The Case of FeS

Anthony Scemama,* Yann Garniron, Michel Caffarel, and Pierre-François Loos*

Laboratoire de Chimie et Physique Quantiques, Université de Toulouse, CNRS, UPS, 31013 Toulouse Cede, France

Supporting Information

ABSTRACT: In diffusion Monte Carlo (DMC) methods, the nodes (or zeroes) of the trial wave function dictate the magnitude of the fixed-node (FN) error. In standard DMC implementations, the nodes are optimized by *stochastically* optimizing a short multideterminant expansion in the presence of an explicitly correlated Jastrow factor. Here, following a recent proposal, we pursue a different route and consider the nodes of selected configuration interaction (sCI) expansions built with the CIPSI (Configuration Interaction using a Perturbative Selection made Iteratively) algorithm. By increasing the size of the sCI expansion, these nodes can be *systematically* and *deterministically* improved. The present methodology is used to investigate the properties of the transition metal sulfide molecule FeS. This apparently simple molecule has been shown to be particularly challenging for electronic structure theory methods due to the proximity of two low-energy quintet electronic states of different spatial symmetry and the difficulty to treat them on equal footing from a one-electron basis set point of view. In particular, we show that, at the triple-ζ basis set level, all sCI results—including those extrapolated at the full CI (FCI) limit—disagree with experiment, yielding an electronic ground state of $^5\Sigma^+$ symmetry. Performing FN-DMC simulation with sCI nodes, we show that the correct $^5\Delta$ ground state is obtained if sufficiently large expansions are used. Moreover, we show that one can systematically get accurate potential energy surfaces and reproduce the experimental dissociation energy as well as other spectroscopic constants.

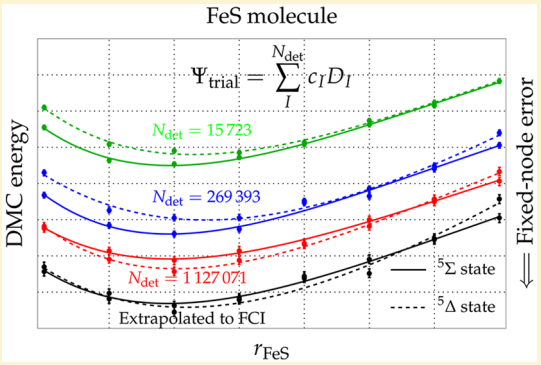

1. INTRODUCTION

From an experimental point of view, transition metal sulfides have proven to be useful in a variety of fields including biological chemistry,[1] catalysis,[2] and electrochemistry.[3] From the computational side, the apparently simple FeS diatomic molecule turns out to be a challenging system for computational chemists. The major hurdle originates from the energetic proximity of two electronic states

$$^5\Delta: \sigma^2\pi^4\sigma^2\delta^3\sigma^1\pi^2 \qquad ^5\Sigma^+: \sigma^2\pi^4\sigma^2\delta^2\sigma^2\pi^2$$

with the same multiplicity competing for the ground state. To make things worse, the equilibrium bond lengths associated with these two states are extremely close to each other.

Experimentally, the ground state of FeS is assigned to be $^5\Delta$,[4,5] with an equilibrium bond length of r_e = 2.017 Å,[5] and a dissociation energy D_0 = 3.31(15) eV.[6] For this state, the harmonic frequency ω_e has been estimated to be 518 ± 5 cm^{-1}.[7] Very recently, a much more accurate value of the dissociation energy D_0 = 3.240(3) eV has been obtained by Matthew et al. using the predissociation threshold technique.[8]

FeS has been extensively studied by density functional theory (DFT) and post-Hartree−Fock methods. In short, most (but not all) DFT functionals correctly predict a $^5\Delta$ ground state,[9−13] while CAS-based multireference methods such as CASSCF/ACPF,[14] CASPT2,[15] or CASSCF/ICACPF[16] systematically predict $^5\Sigma^+$ lower than $^5\Delta$.

Here, we investigate this problem using quantum Monte Carlo (QMC). In recent years, QMC has been applied with great success to a large variety of main group compounds (see, e.g, refs 17−20 for recent applications). Transition metal systems are more challenging, but a number of successful studies have also been reported.[21−41]

When multireference effects are weak, QMC is seen as a very accurate method providing benchmark results of a quality similar or superior to the gold-standard CCSD(T). However, when multireference effects are dominant, as is usually the case for metallic compounds with partially filled d shells, the situation is more complicated, and one has to revert to multireference approaches.[42−44] Indeed, the results may depend significantly on the trial wave function Ψ_T used to guide the walkers through configuration space. In theory, QMC results should be independent of the choice of Ψ_T. However, it is not true in practice because of the fixed-node (FN) approximation, which imposes the Schrödinger equation to be solved with the additional constraint that the solution vanishes at the zeroes (nodes) of the trial wave function. Using an approximate Ψ_T leads to approximate nodes and, thus, to an approximate energy, known as the FN energy. The FN energy being an upper bound of the exact energy, this gives us a

Received: December 14, 2017
Published: January 27, 2018

DOI: 10.1021/acs.jctc.7b01250
J. Chem. Theory Comput. 2018, 14, 1395−1402

practical and convenient variational criterion for characterizing the nodal quality. In situations where multireference effects are strong, getting accurate nodes may be difficult. As we shall see, this is the main challenge we are facing in the present work.

Most QMC studies for transition metal-containing systems have been performed with pseudopotentials. In this case, an additional source of error, the so-called localization error, is introduced. This error, specific to QMC, adds up to the standard error associated with the approximate nature of pseudopotentials. Similarly to the FN error, the localization error depends on Ψ_T and vanishes only for the exact wave function. Therefore, to get accurate and reliable QMC results, both sources of error have to be understood and controlled.

In 2011, Petz and Lüchow reported a FN diffusion Monte Carlo (FN-DMC) study of the energetics of diatomic transition metal sulfides from ScS to FeS using pseudopotentials and single-determinant trial wave functions.[34] The pseudopotential dependence was carefully investigated, and comparisons with both DFT and CCSD(T) as well as experimental data were performed. In short, it was found that FN-DMC shows a higher overall accuracy than both B3LYP and CCSD(T) for all diatomics except for CrS and FeS, which appeared to be particularly challenging.

Very recently, Haghighi-Mood and Lüchow had a second look at the difficult case of FeS.[41] In particular, they explored the impact of the level of optimization on the parameters of multideterminant trial wave functions (partial or full optimization of the Jastrow, determinant coefficients, and molecular orbitals) on both the FN and localization errors. Their main conclusions can be summarized as follows. Using a single-determinant trial wave function made of B3LYP orbitals or fully optimized orbitals in the presence of a Jastrow factor is sufficient to yield the correct state ordering. However, in both cases, the dissociation energy is far from the experimental value, and thus, multideterminant trial wave functions must be employed. Although a natural choice would be to take into account the missing static correlation via a CASSCF-based trial wave function, they showed that it is insufficient and that a full optimization is essential to get both the correct electronic ground state and reasonable estimates of the spectroscopic constants.

In the present study, we revisit this problem within the original QMC protocol developed in our group these past few years.[37,45−49] In the conventional protocol, prevailing in the QMC community and employed by Haghighi-Mood and Lüchow, the nodes of the Slater−Jastrow (SJ) trial wave function

$$\Psi_T^{SJ} = \exp(J)\Psi_{det} \tag{1}$$

are obtained by partially or fully optimizing the Jastrow factor J and the multideterminant expansion Ψ_{det} (containing typically a few hundreds or thousands of determinants). This step is performed in a preliminary variational Monte Carlo calculation by minimizing the energy, the variance of the local energy (or a combination of both), employing one of the optimization methods developed within the QMC context.[50−53] We note that, in practice, the optimization must be carefully monitored because of the large number of parameters (several hundreds or thousands), the nonlinear nature of most parameters (several minima may appear), and the inherent presence of noise in the function to be minimized.

Within our protocol, we rely on configuration interaction (CI) expansions in order to get accurate nodal surfaces, without resorting to the stochastic optimization step. Our fundamental motivation is to take advantage of all of the machinery and experience developed these last decades in the field of wave function methods. In contrast to the standard protocol described above, the CI nodes can be improved *deterministically* and *systematically* by increasing the size of the CI expansion. In the present work, we do not introduce any Jastrow factor, essentially to avoid the expensive numerical quadrature involved in the calculation of the pseudopotential and to facilitate control of the localization error. To keep the size of the CI expansion reasonable and retain only the most important determinants, we propose using selected CI (sCI) algorithms, such as CIPSI (Configuration Interaction using a Perturbative Selection made Iteratively).[45] Using a recently proposed algorithm to handle large numbers of determinants in FN-DMC[47] we are able to consider up to a few million determinants in our simulations.

Over the past few years, we have witnessed a rebirth of sCI methods.[36,37,45−48,54−77] Although these various approaches appear under diverse acronyms, most of them rely on the very same idea of selecting determinants iteratively according to their contribution to the wave function or energy, an idea that goes back to 1969 in the pioneering works of Bender and Davidson,[54] and Whitten and Hackmeyer.[55] Importantly, we note that any sCI variants can be employed here.

The price to pay for using sCI expansions instead of optimized SJ trial wave functions is the need to employ much larger multideterminant expansions in order to reach a comparable level of statistical fluctuations. In practice, a higher computational cost is thus required. Furthermore, because of the absence of an optimized Jastrow factor, systematic errors, such as the time step and basis set incompleteness errors, are larger. Then, in our procedure, it is particularly important to make use of extrapolation procedures for each systematic error. However, these disadvantages are compensated by the appealing features of sCI nodes: (i) they are built in a fully automated way; (ii) they are unique and reproducible; (iii) they can be systematically improved by increasing the level of selection and/or the basis set (with the possibility of complete basis set extrapolation[48]); and (iv) they easily produce smooth potential energy surfaces.[46]

2. COMPUTATIONAL DETAILS

All trial wave functions have been generated with the electronic structure software QUANTUM PACKAGE,[78] while the QMC calculations have been performed with the QMC = CHEM suite of programs.[79,80] Both softwares were developed in our laboratory and are freely available. For all calculations, we used the triple-ζ basis sets of Burkatzki et al.[81,82] (VTZ-ANO-BFD for Fe and VTZ-BFD for S) in conjunction with the corresponding Burkatzki−Filippi−Dolg (BFD) small-core pseudopotentials including scalar relativistic effects. For more details about our implementation of pseudopotentials within QMC, we refer the interested readers to ref 49. As pointed out by Hammond and co-workers,[83] when the trial wave function does not include a Jastrow factor, the nonlocal pseudopotential can be localized analytically and the usual numerical quadrature over the angular part of the nonlocal pseudopotential can be eschewed. In practice, calculation of the localized part of the pseudopotential represents only a small overhead (about 15%) with respect to a calculation without a pseudopotential (and the same number of electrons). To check that the BFD pseudopotentials do not introduce any serious artifact, we

DOI: 10.1021/acs.jctc.7b01250
J. Chem. Theory Comput. 2018, 14, 1395−1402

have computed the nonparallelism error between the frozen-core FCI curves obtained with and without pseudopotentials. A nonparallelism error of 4 mE_h has been observed, which validates the accuracy of these pseudopotentials for the present study.

In order to compare our results for the dissociation energy of FeS with the experimental value of Matthew et al.[8] and the (theoretical) benchmark value of Haghighi-Mood and Lüchow,[41] we have taken into account the zero-point energy (ZPE) correction, the spin−orbit effects as well as the core−valence correlation contribution the same way as those in ref 41. For the $^5\Delta$ state, this corresponds to an increase of the dissociation energy by 0.06 eV and a 0.02 eV stabilization of $^5\Delta$ compared to $^5\Sigma^+$. Unless otherwise stated, atomic units are used throughout.

2.1. Jastrow-Free Trial Wave Functions. Within the spin-free formalism used in QMC, a CI-based trial wave function is written as

$$\Psi_T(\boldsymbol{R}) = \sum_{I=1}^{N_{det}} c_I D_I(\boldsymbol{R}) = \sum_{I=1}^{N_{det}} c_I D_I^{\uparrow}(\boldsymbol{R}^{\uparrow}) D_I^{\downarrow}(\boldsymbol{R}^{\downarrow}) \tag{2}$$

where $\boldsymbol{R} = (\boldsymbol{r}_1, ..., \boldsymbol{r}_N)$ denotes the full set of electronic spatial coordinates, $\boldsymbol{R}^{\uparrow}$ and $\boldsymbol{R}^{\downarrow}$ are the two subsets of spin-up ($\uparrow$) and spin-down ($\downarrow$) electronic coordinates, and $D_I^{\sigma}(\boldsymbol{R}^{\sigma})$ ($\sigma = \uparrow$ or $\downarrow$) are spin-specific determinants.

In practice, the various products $D_I^{\uparrow}D_I^{\downarrow}$ contain many identical spin-specific determinants. For computational efficiency, it is then advantageous to group them and compute only once their contribution to the wave function and its derivatives.[47] Therefore, the Jastrow-free CI trial wave functions employed in the present study are rewritten in a "spin-resolved" form

$$\Psi_T(\boldsymbol{R}) = \sum_{i=1}^{N_{det}^{\uparrow}} \sum_{j=1}^{N_{det}^{\downarrow}} c_{ij} \mathcal{D}_i^{\uparrow}(\boldsymbol{R}^{\uparrow}) \mathcal{D}_j^{\downarrow}(\boldsymbol{R}^{\downarrow}) \tag{3}$$

where $\{\mathcal{D}_i^{\sigma}\}_{i=1,...,N_{det}^{\sigma}}$ denotes the set of all *distinct* spin-specific determinant appearing in eq 2.

2.2. Quantum Monte Carlo Calculations. To avoid handling too many determinants in Ψ_T, a truncation scheme has to be introduced. In most CI and/or QMC calculations, the expansion is truncated by introducing a cutoff either on the CI coefficients or on the norm of the wave function. Here, we use an alternative truncation scheme knowing that most of the computational effort lies in the calculation of the spin-specific determinants and their derivatives. Removing a product of determinants whose spin-specific determinants are already present in other products does not change significantly the computational cost. Accordingly, a natural choice is then to truncate the wave function by removing *independently* spin-up and spin-down determinants. To do so, we decompose the norm of the wave function as

$$\mathcal{N} = \sum_{i=1}^{N_{det}^{\uparrow}} \sum_{j=1}^{N_{det}^{\downarrow}} |c_{ij}|^2 = \sum_{i=1}^{N_{det}^{\uparrow}} \mathcal{N}_i^{\uparrow} = \sum_{j=1}^{N_{det}^{\downarrow}} \mathcal{N}_j^{\downarrow} \tag{4}$$

A determinant $\mathcal{D}_i^{\uparrow}$ is retained in Ψ_T if

$$\mathcal{N}_i^{\uparrow} = \sum_{j=1}^{N_{det}^{\downarrow}} |c_{ij}|^2 > \epsilon \tag{5}$$

where ϵ is a user-defined threshold. A similar formula is used for $\mathcal{D}_j^{\downarrow}$. When $\epsilon = 0$, the entire set of determinants is retained in the QMC simulation.

In order to treat the two electronic states ($^5\Sigma^+$ and $^5\Delta$) on equal footing, a common set of spin-specific determinants $\{\mathcal{D}_i^{\sigma}\}_{i=1,...,N_{det}^{\sigma}}$ is used for both states. In addition, a common set of molecular orbitals issued from a preliminary state-averaged CASSCF calculation is employed. These CASSCF calculations have been performed with the GAMESS, package[84] while for the atoms, we have performed ROHF calculations. The active space contains 12 electrons and 9 orbitals (3d and 4s orbitals of Fe and 3p orbitals of S). The multideterminant expansion (eq 2) has been constructed using the sCI algorithm CIPSI,[56,57] which uses a second-order perturbative criterion to select the energetically important determinants D_I in the FCI space.[36,37,45−48,67] An n_s-state truncated sCI expansion (here $n_s = 2$) is obtained via a natural generalization of the state-specific criterion introduced in eq 5: a determinant $\mathcal{D}_i^{\uparrow}$ is retained in Ψ_T if

$$\mathcal{N}_i^{\uparrow} = \frac{1}{n_s} \sum_{k=1}^{n_s} \sum_{j=1}^{N_{det}^{\downarrow}} |c_{ij}^{(k)}|^2 > \epsilon \tag{6}$$

with a similar formula for $\mathcal{D}_j^{\downarrow}$.

The characteristics of the various trial wave functions considered here (and their acronyms) at $r_{FeS} = 2.0$ Å are presented in Table 1. For other r_{FeS} values, the numbers of determinants are slightly different. Our largest sCI trial wave function contains 8 388 608 determinants and is labeled sCI(∞). The sCI(n) wave functions with $n = 4$, 5, and 6 are obtained by truncation of the sCI(∞) expansion setting $\epsilon = 10^{-n}$. They contain respectively 15 723, 269 393, and 1 127 071 determinants. At this stage, we are not able to use the entire 8 388 608 determinants of the sCI(∞) wave function within our FN-DMC simulations. In comparison, Haghighi-Mood and Lüchow's CASSCF-based trial wave function (labeled as HML in Table 2) only contains 630 and 500 determinants for the $^5\Sigma^+$ and $^5\Delta$ states, respectively.[41] However, as discussed in the Introduction, fully optimized SJ trial wave functions require much smaller multireference expansions.

Table 1. Characteristics of the Various sCI Expansions at r_{FeS} = 2.0 Å for Various Levels of Truncation along with Characteristics of the Extrapolated FCI (exFCI) Expansion

method	ϵ	N_{det}	$N_{det}^{\uparrow}$	$N_{det}^{\downarrow}$	acronym
sCI	10^{-4}	15 723	191	188	sCI(4)
	10^{-5}	269 393	986	1 191	sCI(5)
	10^{-6}	1 127 071	3883	4623	sCI(6)
	0	8 388 608	364 365	308 072	sCI(∞)
exFCI		$\sim 10^{27}$	$\sim 10^{16}$	$\sim 10^{11}$	exFCI

On the basis of these trial wave functions, we performed FN-DMC calculations with the stochastic reconfiguration algorithm developed by Assaraf et al.[85] One of the main advantages of this particular algorithm is that the number of walkers is constant during the simulation, hence avoiding the population control step. Here we have used 100 walkers in our simulations.

In order to remove the time step error, all of our FN-DMC results have been extrapolated to zero time step using a two-point linear extrapolation with $\tau = 2 \times 10^{-4}$ and 4×10^{-4}.[86]

DOI: 10.1021/acs.jctc.7b01250
J. Chem. Theory Comput. 2018, 14, 1395−1402

Table 2. FN-DMC Energies E_{DMC} (in hartrees) at Equilibrium Geometry, Dissociation Energy D_0 (in eV), Equilibrium Distance r_e (in Å), and Harmonic Frequency ω_e (in cm^{-1}) for the $^5\Sigma^+$ and $^5\Delta$ of FeS Obtained with Various Trial Wave Functions Ψ_T[a]

	FeS ($^5\Sigma^+$)			FeS ($^5\Delta$)			Fe (^{5}D)	S (^{3}P)		
Ψ_T	E_{DMC}	r_e	ω_e	E_{DMC}	r_e	ω_e	E_{DMC}	E_{DMC}	D_0	ref
HML	−134.0571(4)	2.00(1)	518(7)	−134.0579(4)	2.031(7)	499(11)	−123.8126(4)	−10.1314(1)	3.159(15)	41
sCI(4)	−134.0101(8)	1.994(7)	532(20)	−134.0040(7)	2.029(7)	502(15)	−123.8028(9)	−10.1279(2)	2.055(20)	this work
sCI(5)	−134.0479(10)	1.992(8)	551(24)	−134.0402(10)	2.048(11)	489(21)	−123.8234(10)	−10.1312(2)	2.389(28)	this work
sCI(6)	−134.061 (14)	1.994(12)	497(35)	−134.0671(14)	2.004(11)	550(32)	−123.8300(12)	−10.1334(3)	3.062(39)	this work
exFCI	−134.0863(15)	1.990(12)	523(37)	−134.0885(18)	2.016(14)	525(40)	−123.8372(12)	−10.1336(3)	3.267(49)	this work
exp.					2.017	518(5)			3.240(3)	5, 7, 8

[a]The error bar corresponding to one standard error is reported in parentheses.

The behavior of the FN-DMC energy as a function of τ is depicted in Figure 1 for various time step values. Note that

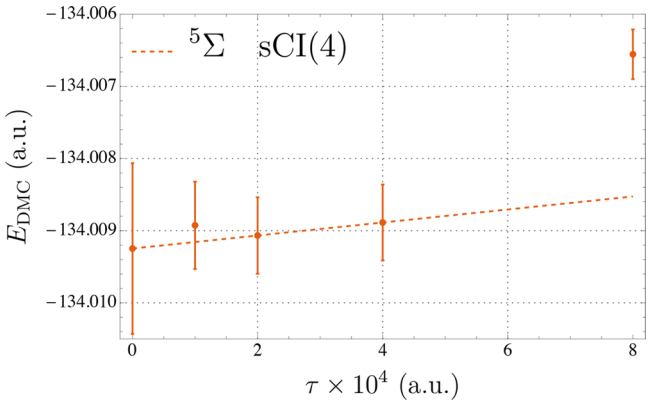

Figure 1. E_{DMC} (in hartrees) for the $^5\Sigma^+$ state of FeS as a function of the time step τ at r_{FeS} = 2.0 Å. The linear extrapolation between $\tau = 2 \times 10^{-4}$ and 4×10^{-4} is represented as a dashed read line. The error bar corresponds to one standard error.

because the variance of the local energy is larger than that in SJ calculations time step errors are enhanced and shorter time steps are required.

2.3. Extrapolation Procedure. In order to extrapolate our sCI results to the FCI limit, we have adopted the method recently proposed by Holmes, Umrigar, and Sharma[76] in the context of the (selected) heat-bath CI method.[72,75,76] It consists of extrapolating the sCI energy E_{sCI} as a function of the second-order Epstein−Nesbet energy

$$E_{PT2} = \sum_{\alpha} \frac{|\langle \alpha|\hat{H}|\Psi_{sCI}\rangle|^2}{E_{sCI} - \langle \alpha|\hat{H}|\alpha\rangle} \tag{7}$$

which is an estimate of the truncation error in the sCI algorithm, i.e, $E_{PT2} \approx E_{FCI} - E_{sCI}$.[56] In eq 7, the sum runs over all external determinants $|\alpha\rangle$ (i.e., not belonging to the sCI expansion) connected via $\hat{H}$ to the sCI wave function Ψ_{sCI}, i.e., $\langle \alpha|\hat{H}|\Psi_{sCI}\rangle \neq 0$. When $E_{PT2} = 0$, the FCI limit has effectively been reached. In our case, E_{PT2} is efficiently evaluated thanks to our recently proposed hybrid stochastic−deterministic algorithm,[67] which explains the presence of an error bar in the numerical values of E_{PT2} gathered in the tables reported in the Supporting Information. The extrapolated FCI results are labeled exFCI from hereon.

3. RESULTS AND DISCUSSION

In Table 2, we report FN-DMC energies at equilibrium geometry as well as other quantities of interest such as the dissociation energy D_0, the equilibrium distance r_e, and the harmonic frequency ω_e obtained with various trial wave functions. These values are obtained via the standard four-parameter Morse potential representation of the numerical values gathered in the Supporting Information. (The error bars have been obtained by fitting a large set of energy curves. Each of these curves is obtained from independent realizations of the statistical noise. Note that due to the absence of correlations in the statistical noise, the error bars obtained in this way are certainly overestimated.) For comparison purposes, Haghighi-Mood and Lüchow's results are also reported based on their best trial wave function.[41] When available, the experimental result is also reported.[5−8] The value of D_0 is always calculated with respect to the $^5\Delta$ state, adding the corresponding corrections for ZPE, spin−orbit effects, and core−valence correlation, as described above (see section 2.1). (The dissociation energies are calculated by treating the atoms and the molecule at the same level of theory, i.e., at the same truncation order.) The dissociation profile of FeS obtained with FN-DMC is depicted in Figure 2 for various trial wave functions.

The first observation we would like to make is that at the variational level the $^5\Delta$ state is never found lower in energy than the $^5\Sigma^+$ state, even after performing extrapolation to the FCI limit. This is illustrated by the left panel of Figure 3, which shows the behavior of the sCI energy as a function of E_{PT2} as well as the extrapolated FCI value The extrapolated value has been obtained via a three-point linear extrapolation of the sCI energy as a function of E_{PT2} using the sCI(5), sCI(6), and sCI(∞) results. (The raw data can be found in the Supporting Information.) It is clear from these results that the $^5\Sigma^+$ and $^5\Delta$ do not cross, even at the FCI limit. Because all post-Hartree−Fock methods are indeed an approximation of FCI, they are expected to predict a $^5\Sigma^+$ ground state for this particular basis set. This observation is in agreement with the CASPT2 results previously published in the literature.[14−16] Thus, one can attribute the wrong state ordering to basis set incompleteness, the only remaining approximation.

To obtain the FN-DMC curve with an *effective* FCI trial wave function, we have generalized the extrapolation procedure described in the previous section, and we have performed a three-point linear extrapolation of the FN-DMC energy as a function of $E_{exFCI} - E_{sCI}$ using the sCI(4), sCI(5), and sCI(6) results (see the right panel of Figure 3). Contrary to the sCI results, at the FN-DMC level, the $^5\Delta$ state does eventually become lower in energy than the $^5\Sigma^+$ state. However, one must include at least a few hundred thousand determinants in order to find the proper ground state. For larger ϵ values (10^{-4} and 10^{-5}), D_0 is underestimated due to the unbalanced treatment of the isolated atoms compared to the dimer at equilibrium

DOI: 10.1021/acs.jctc.7b01250
J. Chem. Theory Comput. 2018, 14, 1395−1402

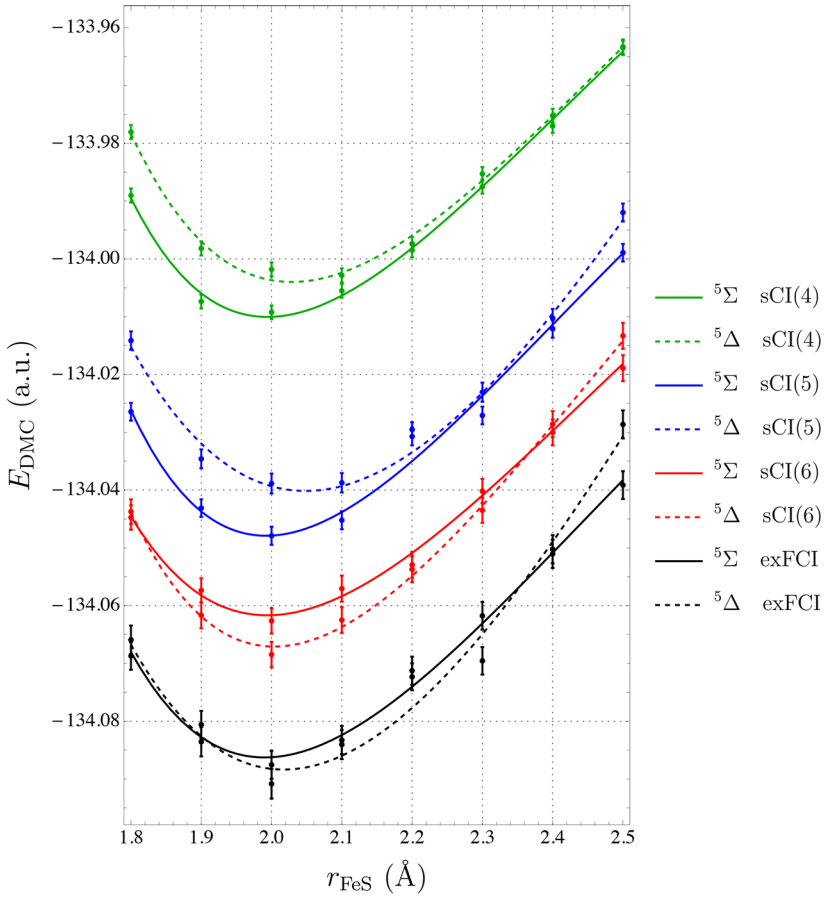

Figure 2. E_{DMC} (in hartrees) for the $^5\Sigma^+$ (solid) and $^5\Delta$ (dashed) states of FeS as a function of r_{FeS} (in Å) for various trial wave functions. The error bar corresponds to one standard error.

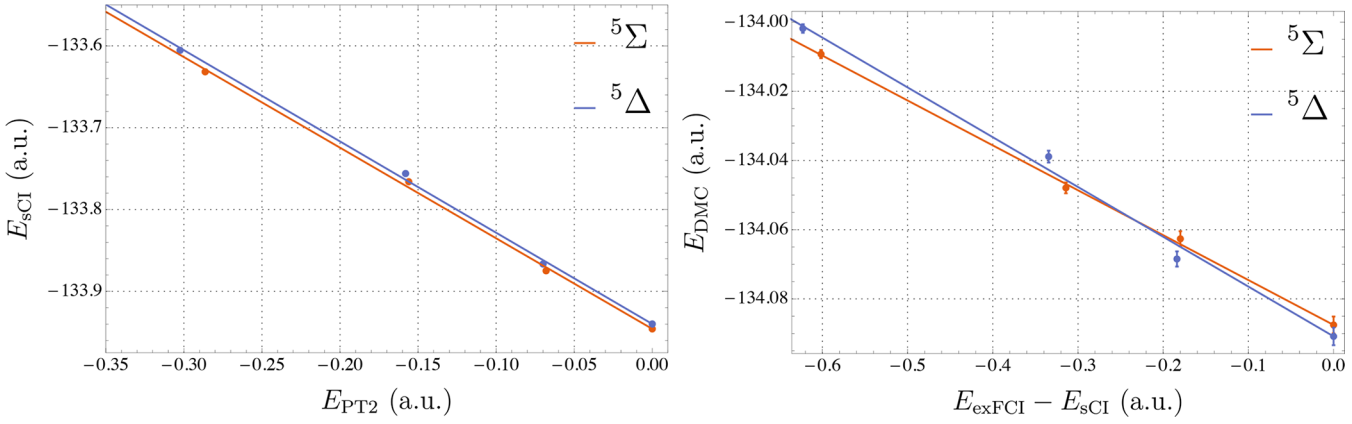

Figure 3. Three-point linear extrapolation of E_{sCI} (left) and E_{DMC} (right) to the FCI limit ($E_{\mathrm{PT2}} = 0$ and $E_{\mathrm{exFCI}} - E_{\mathrm{sCI}} = 0$, respectively) for the $^5\Sigma^+$ (red) and $^5\Delta$ (blue) states of FeS at $r_{\mathrm{FeS}} = 2.0$ Å. The error bar corresponds to one standard error.

geometry. Indeed, for a given number of determinants, the energy of the atomic species is much closer to the FCI limit than the energy of FeS.

For $\epsilon = 10^{-6}$, our approach correctly predicts a $^5\Delta$ ground state. However, although our FN-DMC energies are much lower than those obtained with the HML trial wave function, our estimate of the dissociation energy ($D_0 = 3.062(39)$ eV) is still below the experimental value. This underestimation of D_0 can be ultimately tracked to the lack of size-consistency of the truncated CI wave function. With more than 10^6 determinants in the variational space, the wave function is still 150 mE_{h} higher than the exFCI wave function, while the atoms are much better described by the sCI wave function. To remove the size-consistency error, we then extrapolate the FN-DMC energies to the (size-consistent) FCI limit of the trial wave function, as described above.

In that case, using the extrapolated FN-DMC energies of the molecule and isolated atoms reported in Table 2, we obtain a value of $D_0 = 3.267(49)$ eV, which nestles nicely between the experimental values of Matthew et al.[8] (3.240(3) eV) and Drowart et al.[6] (3.31(15) eV). As a final remark, we note that other spectroscopic constants, such as the equilibrium

DOI: 10.1021/acs.jctc.7b01250
J. Chem. Theory Comput. 2018, 14, 1395−1402

geometry and the harmonic frequency, are fairly well reproduced by our approach. However, increasing the number of determinants in the trial wave function does not systematically improve the equilibrium distances. The same comment can be made for the harmonic frequencies. Overall, we found that our values of ω_e and r_e for the $^5\Delta$ state are closer to the experimental results[5,7] than HML's values.

4. CONCLUSIONS

In this article, the potential energy curves of two electronic states—$^5\Delta$ and $^5\Sigma^+$—of the FeS molecule have been calculated using the sCI algorithm CIPSI and the stochastic FN-DMC method. In all of our sCI calculations, $^5\Sigma^+$ is found to be the ground state, in disagreement with experiment. It is not only true for all CIPSI expansions with up to 8 million determinants but also for the estimated FCI limit obtained using the extrapolation procedure recently proposed by Holmes et al.[76]

This conclusion agrees with other high-level ab initio wave function calculations, which all wrongly predict a ground state of $^5\Sigma^+$ symmetry. FN-DMC calculations have been performed using CIPSI expansions including up to 1 127 071 selected determinants as trial wave functions. Contrary to standard QMC calculations, we do not introduce any Jastrow factor: the CI expansions have been used as they are (no optimization). It is found that, when the number of determinants in the trial wave function reaches a few hundred thousand, the FN-DMC ground state switches from the $^5\Sigma^+$ state to the correct $^5\Delta$ state, as predicted experimentally.

Generalizing the extrapolation procedure of Holmes et al.,[76] an estimate of the FN-DMC potential energy curves corresponding to the FCI nodes can be obtained. The resulting dissociation energy is found to be 3.267(49) eV, in agreement with the recent experimental value of Matthew et al. (3.240(3) eV).[8] As already observed in previous applications, the FN-DMC energy obtained with CIPSI nodes is found to *systematically* decrease as a function of the number of selected determinants.[36,37,45,46,48,49] For the largest expansion, our FN energies are lower than the values recently reported by Haghighi-Mood and Lüchow[41] using a fully optimized SJ trial wave function. This important result illustrates that "pure" sCI nodes are a realistic alternative to stochastically optimized SJ trial wave functions (although more computationally demanding), even for a challenging system such as FeS. A similar conclusion had already been drawn in our recent study of the water molecule.[48]

■ ASSOCIATED CONTENT

Supporting Information

The Supporting Information is available free of charge on the ACS Publications website at DOI: 10.1021/acs.jctc.7b01250.

sCI energies, second-order perturbation corrections, and FN-DMC energy data (PDF)

■ AUTHOR INFORMATION

Corresponding Authors

*E-mail: scemama@irsamc.ups-tlse.fr (A.S.).
*E-mail: loos@irsamc.ups-tlse.fr (P.-F.L.).

ORCID

Pierre-François Loos: 0000-0003-0598-7425

Funding

This work was performed using HPC resources from CALMIP (Toulouse) under Allocation 2016-0510 and from GENCI-TGCC (Grant 2016-08s015).

Notes

The authors declare no competing financial interest.

■ ACKNOWLEDGMENTS

The authors would like to thank Arne Lüchow for numerous stimulating discussions.

■ REFERENCES

(1) Crack, J. C.; Green, J.; Thomson, A. J.; Brun, N. E. L. Iron-Sulfur Clusters as Biological Sensors: The Chemistry of Reactions with Molecular Oxygen and Nitric Oxide. *Acc. Chem. Res.* **2014**, *47*, 3196−3205.

(2) Stiefel, E. I. Transition Metal Sulfur Chemistry: Biological and Industrial Significance and Key Trends. *Trans. Metal Sulfur Chem.* **1996**, *653*, 2−38.

(3) Xiao, S.; Li, X.; Sun, W.; Guan, B.; Wang, Y. General and facile synthesis of metal sulfide nanostructures: In situ microwave synthesis and application as binder-free cathode for Li-ion batteries. *Chem. Eng. J.* **2016**, *306*, 251−259.

(4) Zhang, N.; Hayase, T.; Kawamata, H.; Nakao, K.; Nakajima, A.; Kaya, K. Photoelectron spectroscopy of iron-sulfur cluster anions. *J. Chem. Phys.* **1996**, *104*, 3413−3419.

(5) Takano, S.; Yamamoto, S.; Saito, S. The microwave spectrum of the FeS radical. *J. Mol. Spectrosc.* **2004**, *224*, 137−144.

(6) Drowart, J.; Pattoret, A.; Smoes, S. Mass Spectrometric Studies of the Vaporization of Refractory Compounds. *Proc. Br. Ceram. Soc.* **1967**, *8*, 67−88.

(7) Wang, L.; Huang, D.-l.; Zhen, J.-f.; Zhang, Q.; Chen, Y. Experimental Determination of the Vibrational Constants of FeS(X5) by Dispersed Fluorescence Spectroscopy. *Chin. J. Chem. Phys.* **2011**, *24*, 1−3.

(8) Matthew, D. J.; Tieu, E.; Morse, M. D. Determination of the bond dissociation energies of FeX and NiX (X = C, S, Se). *J. Chem. Phys.* **2017**, *146*, 144310.

(9) Bridgeman, A. J.; Rothery, J. Periodic trends in the diatomic monoxides and monosulfides of the 3d transition metals. *J. Chem. Soc., Dalton Trans.* **2000**, 211−218.

(10) Li, Y.-N.; Wang, S.; Wang, T.; Gao, R.; Geng, C.-Y.; Li, Y.-W.; Wang, J.; Jiao, H. Energies and Spin States of FeS0/, FeS20/, Fe2S20/, Fe3S40/, and Fe4S40/Clusters. *ChemPhysChem* **2013**, *14*, 1182−1189.

(11) Liang, B.; Wang, X.; Andrews, L. Infrared Spectra and Density Functional Theory Calculations of Group 8 Transition Metal Sulfide Molecules. *J. Phys. Chem. A* **2009**, *113*, 5375−5384.

(12) Schultz, N. E.; Zhao, Y.; Truhlar, D. G. Density Functionals for Inorganometallic and Organometallic Chemistry. *J. Phys. Chem. A* **2005**, *109*, 11127−11143.

(13) Wu, Z. J.; Wang, M. Y.; Su, Z. M. Electronic structures and chemical bonding in diatomic ScX to ZnX (X = S, Se, Te). *J. Comput. Chem.* **2007**, *28*, 703−714.

(14) Hübner, O.; Termath, V.; Berning, A.; Sauer, J. A CASSCF/ACPF study of spectroscopic properties of FeS and FeS and the photoelectron spectrum of FeS. *Chem. Phys. Lett.* **1998**, *294*, 37−44.

(15) Clima, S.; Hendrickx, M. F. Photoelectron spectra of FeS explained by a CASPT2 ab initio study. *Chem. Phys. Lett.* **2007**, *436*, 341−345.

(16) Bauschlicher, C. W.; Maître, P. Theoretical study of the first transition row oxides and sulfides. *Theor. Chem. Acc.* **1995**, *90*, 189.

(17) Chen, J.; Zen, A.; Brandenburg, J. G.; Alfè, D.; Michaelides, A. Evidence for stable square ice from quantum Monte Carlo. *Phys. Rev. B: Condens. Matter Mater. Phys.* **2016**, *94*, 220102.

(18) Dubecký, M.; Mitáš, L.; Jurečka, P. Noncovalent Interactions by Quantum Monte Carlo. *Chem. Rev.* **2016**, *116*, 5188−5215.

(19) Zhou, X.; Wang, F. Barrier heights of hydrogen-transfer reactions with diffusion quantum monte carlo method. *J. Comput. Chem.* **2017**, *38*, 798−806.
(20) Guareschi, R.; Zulfikri, H.; Daday, C.; Floris, F. M.; Amovilli, C.; Mennucci, B.; Filippi, C. Introducing QMC/MMpol: Quantum Monte Carlo in Polarizable Force Fields for Excited States. *J. Chem. Theory Comput.* **2016**, *12*, 1674−1683. PMID: 26959751.
(21) Christiansen, P. A. Relativistic effective potentials in transition metal quantum Monte Carlo simulations. *J. Chem. Phys.* **1991**, *95*, 361−363.
(22) Mitáš, L. In *Computer Simulations Studies in Condensed Matter V*; Landau, D. P., Mon, K. K., Schüttler, H. B., Eds.; Springer: Berlin, 1993; p 94.
(23) Belohorec, P.; Rothstein, S. M.; Vrbik, J. Infinitesimal differential diffusion quantum Monte Carlo study of CuH spectroscopic constants. *J. Chem. Phys.* **1993**, *98*, 6401−6405.
(24) Mitáš, L. Quantum Monte Carlo calculation of the Fe atom. *Phys. Rev. A: At., Mol., Opt. Phys.* **1994**, *49*, 4411−4414.
(25) Sokolova, S.; Lüchow, A. An ab initio study of TiC with the diffusion quantum Monte Carlo method. *Chem. Phys. Lett.* **2000**, *320*, 421−424.
(26) Wagner, L.; Mitáš, L. A quantum Monte Carlo study of electron correlation in transition metal oxygen molecules. *Chem. Phys. Lett.* **2003**, *370*, 412−417.
(27) Diedrich, C.; Lüchow, A.; Grimme, S. Performance of diffusion Monte Carlo for the first dissociation energies of transition metal carbonyls. *J. Chem. Phys.* **2005**, *122*, 021101.
(28) Caffarel, M.; Daudey, J.-P.; Heully, J.-L.; Ramírez-Solís, A. Towards accurate all-electron quantum Monte Carlo calculations of transition-metal systems: Spectroscopy of the copper atom. *J. Chem. Phys.* **2005**, *123*, 094102.
(29) Buendía, E.; Gálvez, F.; Sarsa, A. Correlated wave functions for the ground state of the atoms Li through Kr. *Chem. Phys. Lett.* **2006**, *428*, 241−244.
(30) Wagner, L. K.; Mitáš, L. Energetics and dipole moment of transition metal monoxides by quantum Monte Carlo. *J. Chem. Phys.* **2007**, *126*, 034105.
(31) Bande, A.; Lüchow, A. Vanadium oxide compounds with quantum Monte Carlo. *Phys. Chem. Chem. Phys.* **2008**, *10*, 3371.
(32) Casula, M.; Marchi, M.; Azadi, S.; Sorella, S. A consistent description of the iron dimer spectrum with a correlated single-determinant wave function. *Chem. Phys. Lett.* **2009**, *477*, 255−258.
(33) Bouabça, T.; Braïda, B.; Caffarel, M. Multi-Jastrow trial wavefunctions for electronic structure calculations with quantum Monte Carlo. *J. Chem. Phys.* **2010**, *133*, 044111.
(34) Petz, R.; Lüchow, A. Energetics of Diatomic Transition Metal Sulfides ScS to FeS with Diffusion Quantum Monte Carlo. *ChemPhysChem* **2011**, *12*, 2031−2034.
(35) Buendía, E.; Gálvez, F.; Maldonado, P.; Sarsa, A. Quantum Monte Carlo ionization potential and electron affinity for transition metal atoms. *Chem. Phys. Lett.* **2013**, *559*, 12−17.
(36) Caffarel, M.; Giner, E.; Scemama, A.; Ramírez-Solís, A. Spin Density Distribution in Open-Shell Transition Metal Systems: A Comparative Post-Hartree-Fock, Density Functional Theory, and Quantum Monte Carlo Study of the CuCl2Molecule. *J. Chem. Theory Comput.* **2014**, *10*, 5286−5296.
(37) Scemama, A.; Applencourt, T.; Giner, E.; Caffarel, M. Accurate nonrelativistic ground-state energies of 3d transition metal atoms. *J. Chem. Phys.* **2014**, *141*, 244110.
(38) Trail, J. R.; Needs, R. J. Correlated electron pseudopotentials for 3d-transition metals. *J. Chem. Phys.* **2015**, *142*, 064110.
(39) Doblhoff-Dier, K.; Meyer, J.; Hoggan, P. E.; Kroes, G.-J.; Wagner, L. K. Diffusion Monte Carlo for Accurate Dissociation Energies of 3d Transition Metal Containing Molecules. *J. Chem. Theory Comput.* **2016**, *12*, 2583−2597.
(40) Krogel, J. T.; Santana, J. A.; Reboredo, F. A. Pseudopotentials for quantum Monte Carlo studies of transition metal oxides. *Phys. Rev. B: Condens. Matter Mater. Phys.* **2016**, *93*, 075143.
(41) Haghighi Mood, K.; Lüchow, A. Full Wave Function Optimization with Quantum Monte Carlo and Its Effect on the Dissociation Energy of FeS. *J. Phys. Chem. A* **2017**, *121*, 6165−6171.
(42) Giner, E.; David, G.; Scemama, A.; Malrieu, J. P. A simple approach to the state-specific MR-CC using the intermediate Hamiltonian formalism. *J. Chem. Phys.* **2016**, *144*, 064101.
(43) Giner, E.; Angeli, C.; Garniron, Y.; Scemama, A.; Malrieu, J.-P. A Jeziorski-Monkhorst fully uncontracted multi-reference perturbative treatment. I. Principles, second-order versions, and tests on ground state potential energy curves. *J. Chem. Phys.* **2017**, *146*, 224108.
(44) Garniron, Y.; Giner, E.; Malrieu, J.-P.; Scemama, A. Alternative definition of excitation amplitudes in multi-reference state-specific coupled cluster. *J. Chem. Phys.* **2017**, *146*, 154107.
(45) Giner, E.; Scemama, A.; Caffarel, M. Using perturbatively selected configuration interaction in quantum Monte Carlo calculations. *Can. J. Chem.* **2013**, *91*, 879−885.
(46) Giner, E.; Scemama, A.; Caffarel, M. Fixed-node diffusion Monte Carlo potential energy curve of the fluorine molecule F2 using selected configuration interaction trial wavefunctions. *J. Chem. Phys.* **2015**, *142*, 044115.
(47) Scemama, A.; Applencourt, T.; Giner, E.; Caffarel, M. Quantum Monte Carlo with very large multideterminant wavefunctions. *J. Comput. Chem.* **2016**, *37*, 1866−1875.
(48) Caffarel, M.; Applencourt, T.; Giner, E.; Scemama, A. Communication: Toward an improved control of the fixed-node error in quantum Monte Carlo: The case of the water molecule. *J. Chem. Phys.* **2016**, *144*, 151103.
(49) Caffarel, M.; Applencourt, T.; Giner, E.; Scemama, A. *ACS Symp. Ser.* **2016**, *1234*, 15−46.
(50) Umrigar, C. J.; Filippi, C. Energy and Variance Optimization of Many-Body Wave Functions. *Phys. Rev. Lett.* **2005**, DOI: 10.1103/PhysRevLett.94.150201.
(51) Toulouse, J.; Umrigar, C. J. Optimization of quantum Monte Carlo wave functions by energy minimization. *J. Chem. Phys.* **2007**, *126*, 084102.
(52) Umrigar, C. J.; Toulouse, J.; Filippi, C.; Sorella, S.; Hennig, R. G. Alleviation of the Fermion-Sign Problem by Optimization of Many-Body Wave Functions. *Phys. Rev. Lett.* **2007**, DOI: 10.1103/PhysRevLett.98.110201.
(53) Toulouse, J.; Umrigar, C. J. Full optimization of Jastrow-Slater wave functions with application to the first-row atoms and homonuclear diatomic molecules. *J. Chem. Phys.* **2008**, *128*, 174101.
(54) Bender, C. F.; Davidson, E. R. Studies in Configuration Interaction: The First-Row Diatomic Hydrides. *Phys. Rev.* **1969**, *183*, 23−30.
(55) Whitten, J. L.; Hackmeyer, M. Configuration Interaction Studies of Ground and Excited States of Polyatomic Molecules. I. The CI Formulation and Studies of Formaldehyde. *J. Chem. Phys.* **1969**, *51*, 5584−5596.
(56) Huron, B.; Malrieu, J. P.; Rancurel, P. Iterative perturbation calculations of ground and excited state energies from multiconfigurational zeroth order wavefunctions. *J. Chem. Phys.* **1973**, *58*, 5745−5759.
(57) Evangelisti, S.; Daudey, J.-P.; Malrieu, J.-P. Convergence of an improved CIPSI algorithm. *Chem. Phys.* **1983**, *75*, 91−102.
(58) Cimiraglia, R. Second order perturbation correction to CI energies by use of diagrammatic techniques: An improvement to the CIPSI algorithm. *J. Chem. Phys.* **1985**, *83*, 1746−1749.
(59) Cimiraglia, R.; Persico, M. Recent advances in multireference second order perturbation CI: The CIPSI method revisited. *J. Comput. Chem.* **1987**, *8*, 39−47.
(60) Illas, F.; Rubio, J.; Ricart, J. M. Approximate natural orbitals and the convergence of a second order multireference many body perturbation theory (CIPSI) algorithm. *J. Chem. Phys.* **1988**, *89*, 6376−6384.
(61) Povill, A.; Rubio, J.; Illas, F. Treating large intermediate spaces in the CIPSI method through a direct selected CI algorithm. *Theor. Chem. Acc.* **1992**, *82*, 229−238.

DOI: 10.1021/acs.jctc.7b01250
J. Chem. Theory Comput. 2018, 14, 1395−1402

(62) Abrams, M. L.; Sherrill, C. D. Important configurations in configuration interaction and coupled-cluster wave functions. *Chem. Phys. Lett.* **2005**, *412*, 121−124.
(63) Bunge, C. F.; Carbó-Dorca, R. Select-divide-and-conquer method for large-scale configuration interaction. *J. Chem. Phys.* **2006**, *125*, 014108.
(64) Bytautas, L.; Ruedenberg, K. A priori identification of configurational deadwood. *Chem. Phys.* **2009**, *356*, 64−75.
(65) Booth, G. H.; Thom, A. J. W.; Alavi, A. Fermion Monte Carlo without fixed nodes: A game of life, death, and annihilation in Slater determinant space. *J. Chem. Phys.* **2009**, *131*, 054106.
(66) Knowles, P. J. Compressive sampling in configuration interaction wavefunctions. *Mol. Phys.* **2015**, *113*, 1655−1660.
(67) Garniron, Y.; Scemama, A.; Loos, P.-F.; Caffarel, M. Hybrid stochastic-deterministic calculation of the second-order perturbative contribution of multireference perturbation theory. *J. Chem. Phys.* **2017**, *147*, 034101.
(68) Evangelista, F. A. Adaptive multiconfigurational wave functions. *J. Chem. Phys.* **2014**, *140*, 124114.
(69) Liu, W.; Hoffmann, M. R. iCI: Iterative CI toward full CI. *J. Chem. Theory Comput.* **2016**, *12*, 1169−1178.
(70) Schriber, J. B.; Evangelista, F. A. Communication: An adaptive configuration interaction approach for strongly correlated electrons with tunable accuracy. *J. Chem. Phys.* **2016**, *144*, 161106.
(71) Tubman, N. M.; Lee, J.; Takeshita, T. Y.; Head-Gordon, M.; Whaley, K. B. A deterministic alternative to the full configuration interaction quantum Monte Carlo method. *J. Chem. Phys.* **2016**, *145*, 044112.
(72) Holmes, A. A.; Tubman, N. M.; Umrigar, C. J. Heat-Bath Configuration Interaction: An Efficient Selected Configuration Interaction Algorithm Inspired by Heat-Bath Sampling. *J. Chem. Theory Comput.* **2016**, *12*, 3674−3680.
(73) Per, M. C.; Cleland, D. M. Energy-based truncation of multi-determinant wavefunctions in quantum Monte Carlo. *J. Chem. Phys.* **2017**, *146*, 164101.
(74) Ohtsuka, Y.; Hasegawa, J.-y Selected configuration interaction method using sampled first-order corrections to wave functions. *J. Chem. Phys.* **2017**, *147*, 034102.
(75) Sharma, S.; Holmes, A. A.; Jeanmairet, G.; Alavi, A.; Umrigar, C. J. Semistochastic Heat-Bath Configuration Interaction Method: Selected Configuration Interaction with Semistochastic Perturbation Theory. *J. Chem. Theory Comput.* **2017**, *13*, 1595−1604.
(76) Holmes, A. A.; Umrigar, C. J.; Sharma, S. Excited states using semistochastic heat-bath configuration interaction. *J. Chem. Phys.* **2017**, *147*, 164111.
(77) Zimmerman, P. M. Incremental full configuration interaction. *J. Chem. Phys.* **2017**, *146*, 104102.
(78) Scemama, A.; Applencourt, T.; Garniron, Y.; Giner, E.; David, G.; Caffarel, M. *Quantum Package* v1.0. https://github.com/LCPQ/quantum_package (2016).
(79) Scemama, A.; Giner, E.; Applencourt, T.; Caffarel, M. *QMC = Chem*. https://github.com/scemama/qmcchem (2017).
(80) Scemama, A.; Caffarel, M.; Oseret, E.; Jalby, W. Quantum Monte Carlo for large chemical systems: Implementing efficient strategies for petascale platforms and beyond. *J. Comput. Chem.* **2013**, *34*, 938−951.
(81) Burkatzki, M.; Filippi, C.; Dolg, M. Energy-consistent pseudopotentials for quantum Monte Carlo calculations. *J. Chem. Phys.* **2007**, *126*, 234105.
(82) Burkatzki, M.; Filippi, C.; Dolg, M. Energy-consistent small-core pseudopotentials for 3d-transition metals adapted to quantum Monte Carlo calculations. *J. Chem. Phys.* **2008**, *129*, 164115.
(83) Hammond, B. L.; Reynolds, P. J.; Lester, W. A. Valence quantum Monte Carlo with ab initio effective core potentials. *J. Chem. Phys.* **1987**, *87*, 1130−1136.
(84) Schmidt, M. W.; Baldridge, K. K.; Boatz, J. A.; Elbert, S. T.; Gordon, M. S.; Jensen, J. H.; Koseki, S.; Matsunaga, N.; Nguyen, K. A.; Su, S.; et al. General atomic and molecular electronic structure system. *J. Comput. Chem.* **1993**, *14*, 1347−1363.
(85) Assaraf, R.; Caffarel, M.; Khelif, A. Diffusion Monte Carlo methods with a fixed number of walkers. *Phys. Rev. E: Stat. Phys., Plasmas, Fluids, Relat. Interdiscip. Top.* **2000**, *61*, 4566−4575.
(86) Lee, R. M.; Conduit, G. J.; Nemec, N.; López Ríos, P.; Drummond, N. D. Strategies for improving the efficiency of quantum Monte Carlo calculations. *Phys. Rev. E* **2011**, *83*, 066706.

DOI: 10.1021/acs.jctc.7b01250
J. Chem. Theory Comput. 2018, 14, 1395−1402